doi:10.3772/j.issn.1006-6748.2021.01.001

Experimental study of suppressing the unbalanced response vibration of rotor system with a G-type integral squeeze film damper①

Yan Wei(闫 伟), He Lidong②, Zhang Yufei, Zhang Yipeng, Jia Xingyun
(Beijing Key Laboratory of Health Monitoring and Self-Recovery for High-End Mechanical Equipment, Beijing University of Chemical Technology, Beijing 100029, P. R. China)

Abstract

Conventional squeeze film dampers have numerous challenges including lock up, bistable response and incoordinate precession. In order to resolve these nonlinear problems, a novel G-type integral squeeze film damper (GISFD) is proposed in this research. The experimental test rig is provided to investigate the rotor system with an unbalanced single disk. Numerical simulation results show that the structural design of GISFD is reasonable, which can ensure its safe and stable operation. The influence of different support stiffnesses on the first-order speed of the rotor system is analyzed. Experimental results show that GISFD can effectively suppress the unbalanced response vibration of the rotor. In a certain range, it is found that the suppression effect of GISFD increases with the increase in the kinematic viscosity of the damping fluid. When the silicone oil with kinematic viscosity coefficients $v = 30.0\ \mathrm{cm^2/s}$ is employed, the vibration reduction of GISFD is approximately 71.51%. Furthermore, the experimental results show that with the increase of the unbalance, there is a linear relationship between the unbalance and the corresponding amplitude of the unbalanced response. It is concluded that GISFD has excellent linear damping characteristics and reduces the sensitivity of the rotor system to the unbalanced mass.

Key words: G-type integral squeeze film damper (GISFD), unbalanced response, vibration suppression, rotor system, dynamic characteristic

0 Introduction

With development in the field of advanced turbomachinery, rotating machines such as aeroengines, turbopumps and heavy-duty gas turbines are widely applied in diverse industrial applications. These machines have supercritical flexible rotors, which inevitably produce remarkable vibration when the shaft speed exceeds the critical speed prior to reach the operating speed. Studies show that such vibrations mainly originate from the unbalanced mass[1]. The squeeze film damper is applied to effectively improve the rotor system damping so that the unbalanced response vibration of the rotor is reduced[1-2]. Several types of squeeze film damper, including the squeeze film damper (SFD), porous ring squeeze film damper (PRSFD) and the elastic ring squeeze film damper (ERSFD), have been proposed. Among them, the combination of squirrel cage elastic support and elastic ring squeeze film damper has been applied to АЛ-31Ф engine in Russia, which effectively reduced the engine vibration.

Recently, Ref. [3] showed that there are two stable periodic responses in the experimental study of the unbalanced response of the squeeze film damper rotor system. Ref. [4] found the same phenomenon in the experiment of the unbalanced response of the squeeze film damper rotor system. Experimental results showed that for excessive unbalances, the hard spring effect is produced, which makes the jump phenomenon of the rotor subsystem. These results showed that the jump phenomenon originates from the highly nonlinear oil film stiffness in the squeeze film damper. Moreover, Ref. [1] proved that the jump phenomenon appears when the cross stiffness of the system increases. These results showed that such increment originates from the acceleration of the annular flow of the oil film because of the vibration. Ref. [5] found that when the operating speed is more than twice of the first-order speed, subharmonic motions appear in the rotor system. Refs[6-8]

① Supported by the National Science and Technology Major Project (No. 2017-Ⅳ-0010-0047) and the Fundamental Research Funds for the Central Universities (No. JD2003).
② To whom correspondence should be addressed. E-mail: 1963he@163.com
Received on July 1, 2020

carried out numerical simulations on the unbalanced response of the rigid rotor supported by the squeeze film damper. These results showed that for large unbalances and eccentricity ratios, the system has subharmonic, quasi-periodic and even chaotic vibration. Some analyses have pointed out that the damping force produced by SFD is a nonlinear function of the journal amplitude. When there are severe conditions such as large load and abrupt unbalance, which are beyond the design range, phenomena such as bistable rotor response, locking and non-coordinated precession are probable[9-10].

In order to improve the nonlinearity of oil film forces in the SFD, many new types of squeeze film dampers such as floating-ring squeeze film dampers (FSFD) and hybrid squeeze film damper (HSFD)[11-15] have been proposed recently. Ref. [16] proposed a new type of shear viscous damper for rotating machinery. The experimental results show that the damper can effectively suppress the misalignment vibration of the rotor system. Refs[17-18] explored the effect of semi-active MR damper on the dynamic characteristics of the rotor system. These results show that the damper has better damping performance and improves the stability of the system. Refs[19-20] combined the active magnetic bearing (AMB) technology with the conventional bearing to control the subsynchronous vibration of single disk rotor. The research shows that the amplitude of subsynchronous vibration can be reduced by 93%. However, these dampers have complex structure and assembly conditions, and need a lot of experimental researches to verify their stability. These dampers are difficult to be applied in engineering.

In order to suppress the vibration of the unbalanced response of the rotor system and improve the nonlinear problems of SFD, a novel G-type integral squeeze film damper (GISFD) is proposed. GISFD has both the low stiffness characteristics in the elastic support and the high damping characteristics in the squeeze film damper. GISFD can effectively suppress the rotor vibration and improve the stability of the rotor system. Moreover, GISFD has the superiorities, including small size and weight, simple structure, easy to inspection and maintenance.

In this research, GISFD with required stiffness is designed. The finite element analysis of GISFD ensures the rationality of its structure design. In addition, a test rig consisting of the single disk rotor system supported by GISFD is built to study the unbalanced response of the rotor, to explore the mechanism of GISFD suppressing the unbalanced response vibration of the rotor system when GISFD is filled with different viscosity damping fluids. Meantime, the variations of the unbalanced response of the rotor system with GISFD at different unbalanced conditions are investigated.

1 G-type integral squeeze film damper

The structure of the GISFD is shown in Fig. 1. GISFD is mainly composed of 4 parts: inner race, outer race, squeeze film area and the G-type elastomer. The inner and outer races are connected by 4 G-type elastomers, which determine the radial static stiffness coefficient of the damper. The gap between the inner and outer races is the squeeze film area. The damping fluid in this area produces the squeeze film effect under the squeeze action, providing stable damping force for the rotor system to dissipate the vibration energy.

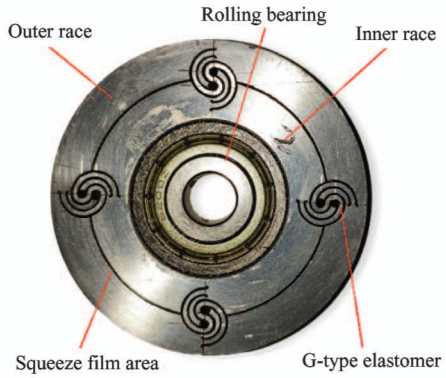

Fig. 1 Configuration of GISFD with a rolling bearing

Fig. 1 illustrates the configuration of GISFD with a rolling bearing. The inner race of GISFD and the outer ring of the rolling bearing are interference fit. The outer race of GISFD is installed and fixed in the bearing block. The basic parameters of GISFD structure are listed in Table 1.

Table 1 Critical structure parameters in GISFD

Parameter	Value
Axial length/mm	10
Inner diameter/mm	30
Outer diameter/mm	60
Oil film radius/mm	22.5
Oil film clearance/mm	0.2
G-shaped elastomer height/mm	10.8

1.1 Equivalent physical model of GISFD

The damping force generated by the extruded oil film in GISFD can be linearized, and the equivalent physical model of GISFD can be observed in Fig. 2. K_{ij} and C_{ij} are the stiffness and damping coefficient of the

equivalent physical model, where i and j respectively represent x- and y- directions. Different stiffness and damping magnitudes can be obtained by altering GISFD axial length, G-shaped elastomer height, oil film radius and oil film clearance.

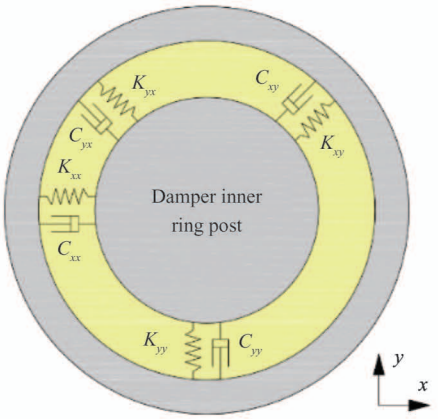

Fig. 2 Equivalent physical model of GISFD[21]

1.2 Finite element analysis of GISFD

Since the stiffness coefficient of GISFD is closely related to the structural parameters of G-type elastomer, dampers with different stiffness coefficients can be obtained by changing the shape and thickness of the G-type elastomer. To calculate the design stiffness coefficient of the damper and determine whether or not there is stress concentration in the structure, the static analysis is performed on the designed GISFD. Fig. 3 shows the displacement and stress contour accordingly. Fig. 3(a) indicates that the design stiffness coefficient of GISFD is 1.4×10^6 N/m. Moreover, the stress contour in Fig. 3(b) shows that there is no obvious stress concentration in the G-type elastomer of the damper, which proves that the structural design of the damper is reasonable, and the safe and stable operation is ensured.

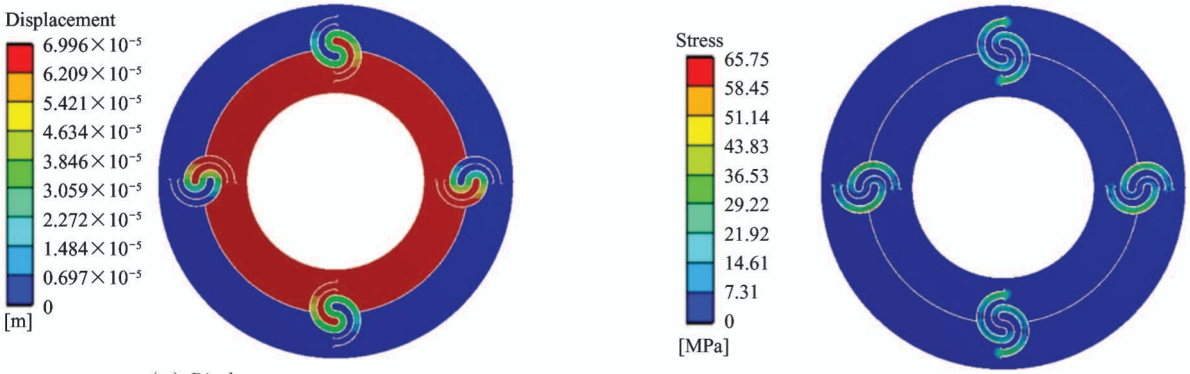

(a) Displacement contour (b) Stress contour

Fig. 3 Contours of GISFD static analysis under a loading of 100 N

2 Dynamic model of the rotor system

The following assumptions are proposed to obtain the model: (1) this is an elastic massless shaft; (2) the axial length of the disk is ignored, and the unbalanced mass of the disk is in a plane; (3) the influence of the torsional vibration of the shaft on the angular velocity is ignored; (4) the stiffness and damping of GISFD are isotropic. Based on these assumptions, dynamic models of the rigid support and GISFD supported rotor systems with an unbalanced single disk are established, providing a theoretical basis for experimental research.

2.1 Dynamic model of rigid support rotor

A schematic diagram of the rigid support rotor system with an unbalanced single disk is established, as shown in Fig. 4. The two ends of the rotor adopt a rigid support structure, which is composed of a bearing block, a rigid sleeve, and a rolling bearing.

It is assumed that the lateral displacements of the geometric center of the disk in the x- and y-directions are presented by x_D and y_D, respectively. Moreover, m_D, k_S and c_S denote the equivalent concentrated mass of the disk, stiffness coefficient and damping coefficient of the rotor, respectively. e_μ is the unbalanced mass eccentricity of the disk, ω is the angular velocity of the rotor. Furthermore, m_B, k_B and c_B are the equivalent concentrated mass, stiffness coefficient and damping coefficient of the rolling bearing, respectively. The (x_B, y_B) is the displacement of the journal of the rolling bearing. The dynamic differential equation of the rotor system can be expressed as:

$$\begin{cases} m_D\ddot{x}_D + 2c_S(\dot{x}_D - \dot{x}_B) + 2k_S(x_D - x_B) = m_D e_\mu \omega^2 \cos\omega t \\ m_D\ddot{y}_D + 2c_S(\dot{y}_D - \dot{y}_B) + 2k_S(y_D - y_B) = m_D e_\mu \omega^2 \sin\omega t - m_D g \\ m_B\ddot{x}_B + c_B\dot{x}_B + k_B x_B = c_S(\dot{x}_D - \dot{x}_B) + k_S(x_D - x_B) \\ m_B\ddot{y}_B + c_B\dot{y}_B + k_B y_B = c_S(\dot{y}_D - \dot{y}_B) + k_S(y_D - y_B) \end{cases} \tag{1}$$

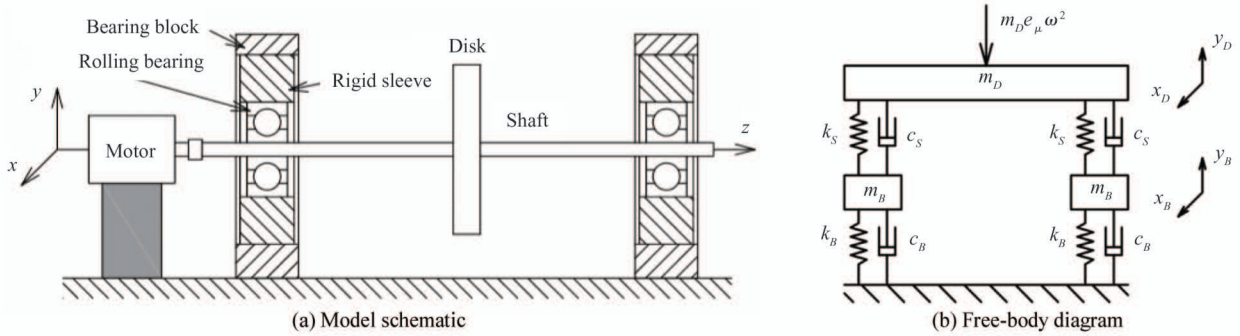

Fig. 4 Dynamic model of the rotor system supported on rolling bearings with the rigid sleeve

2.2 Dynamic model of GISFD supported rotor

A schematic diagram of the GISFD supported rotor system with an unbalanced single disk is established, as shown in Fig. 5. Both ends of the rotor adopt a GISFD support structure, which consists of a bearing block, a GISFD, and a rolling bearing. The displacements of GISFD in the x- and y-directions are presented by x_I and y_I, respectively. Moreover, m_I, k_I and c_I denote the equivalent concentrated mass, stiffness coefficient and damping coefficient of GISFD, respectively.

The dynamic differential equation of the rotor system can be expressed as follows.

$$\begin{cases} m_D\ddot{x}_D + 2c_S(\dot{x}_D - \dot{x}_B) + 2k_S(x_D - x_B) = m_D e_\mu \omega^2 \cos\omega t \\ m_D\ddot{y}_D + 2c_S(\dot{y}_D - \dot{y}_B) + 2k_S(y_D - y_B) = m_D e_\mu \omega^2 \sin\omega t - m_D g \\ m_B\ddot{x}_B + c_B(\dot{x}_B - \dot{x}_I) + k_B(x_B - x_I) = c_S(\dot{x}_D - \dot{x}_B) + k_S(x_D - x_B) \\ m_B\ddot{y}_B + c_B(\dot{y}_B - \dot{y}_I) + k_B(y_B - y_I) = c_S(\dot{y}_D - \dot{y}_B) + k_S(y_D - y_B) \\ m_I\ddot{x}_I + c_I\dot{x}_I + k_I x_I = c_B(\dot{x}_B - \dot{x}_I) + k_B(x_B - x_I) \\ m_I\ddot{y}_I + c_I\dot{y}_I + k_I y_I = c_B(\dot{y}_B - \dot{y}_I) + k_B(y_B - y_I) \end{cases} \tag{2}$$

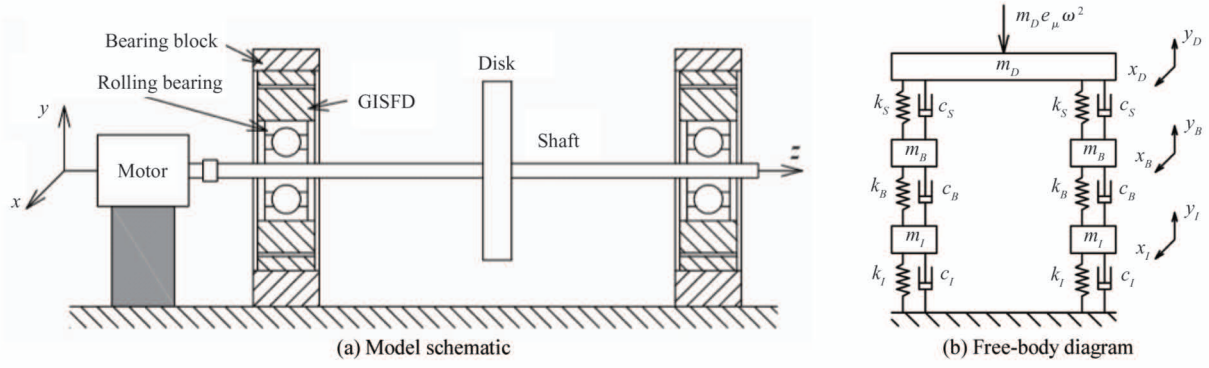

Fig. 5 Dynamic model of the rotor system supported on rolling bearings with the GISFD

3 Introduction of experimental test rig

In order to investigate the influence of GISFD on the unbalanced response of the rotor system and evaluate the corresponding vibration reduction performance, a test rig is established for the rotor system with an unbalanced single disk. Fig. 6 presents schematic configuration of the test rig. Comparing the vibration changes of the unbalanced response of the rotor with the rigid sleeve and the GISFD in the bearing block, the vibration reduction performance of GISFD is studied and verified.

The experimental platform of the unbalanced rotor system mainly consists of the vibration signal acquisition system and the rotor system with an unbalanced

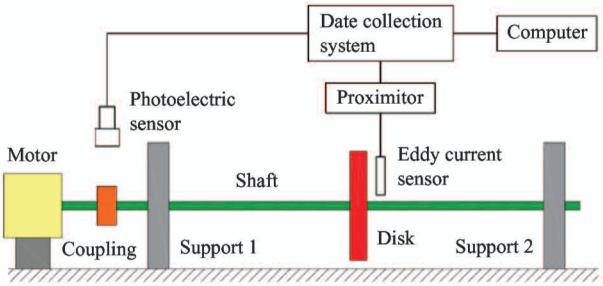

Fig. 6 Experimental test rig of the rotor system with an unbalanced single disk

single disk. Moreover, the vibration signal acquisition system is mainly composed of the photoelectric sensor, eddy current sensor, proximitor, date collection system and a computer. During the experiments, the photoelectric sensor probes the rotor speed, while the eddy current sensor collects the vibration displacement of the rotor near the disk. Then the date collection system transmits the measured data to the computer for recording and saving.

The unbalanced single disk rotor system mainly consists of the following parts.

(1) Disk. Table 2 lists the material parameters of the disk. There are 16 evenly distributed counterweight holes on the disk, and the counterweight radius is 30 mm. The disk can be equipped with different unbalanced masses in the counterweight holes.

(2) Shaft and support. Table 2 lists the material parameters of the shaft. There are two support types. By replacing the GISFD and the rigid sleeve in the bearing block, experiments are conducted to study the rotor system with GISFD support and rigid support. Fig. 7 illustrates the installation diagram of two type supports. Fig. 7(a) shows the rigid support, which is the traditional support configuration, consisting of a rigid sleeve, a rolling bearing, a bearing block, end covers, and rubber O-rings. Fig. 7(b) shows the GISFD support consisting of a GISFD, a rolling bearing, a bearing block, end covers, and rubber O-rings. It is observed that the GISFD is installed between the bearing outer ring and the bearing block. It should be indicated that the rigid sleeve is a rigid ring with the same size and material as the damper.

Table 2 Structural and material parameters of the rotor system

Parameter	Value
Disk diameter/mm	75
Disk thickness/mm	15
Disk mass/g	503
Shaft diameter/mm	10
Shaft length/mm	600
Shaft span/mm	420

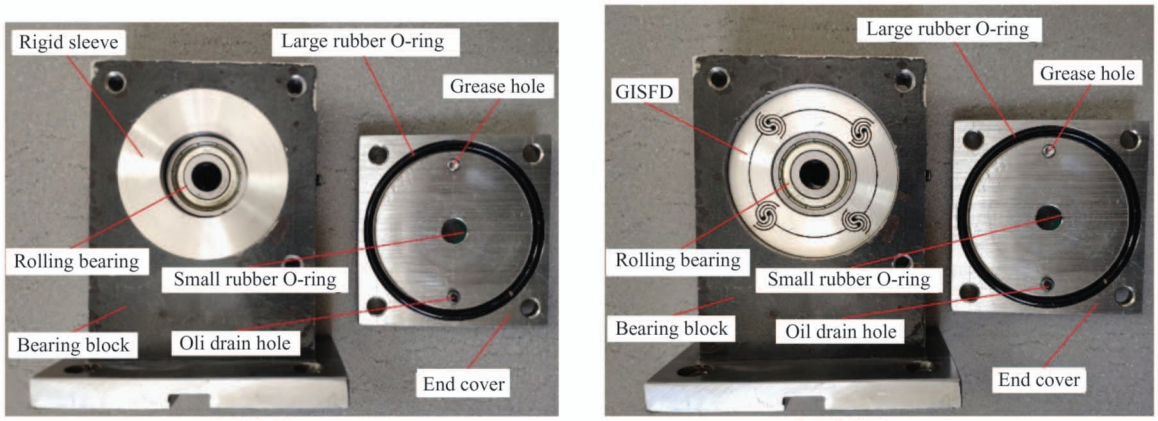

Fig. 7 Configuration of two supports with no damper and GISFD

(3) Drive motor and coupling. The driving motor used in the experiment is a servomotor with permanent DC magnet, which can realize stepless speed regulation of 0 – 10 000 rpm. During the experiment, the drive motor and the shaft are connected through a flexible coupling to realize the continuous rotation of the shaft.

Fig. 8 illustrates the configuration of the experimental test rig in this research. It should be indicated that the rotor system was dynamically balanced prior to the experiment to minimize the residual unbalance.

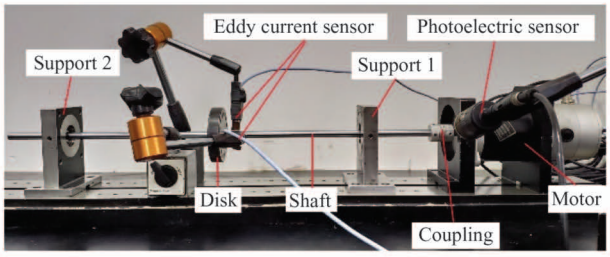

Fig. 8 Configuration of experimental test rig for unbalanced rotor system

During the experiment, photoelectric sensor monitors the rotational speed of rotor, while the eddy current sensor probes the vertical and horizontal displacement vibration of the shaft near the disk.

4 Results and discussion

4.1 Effect of the support stiffness on the first-order speed of the rotor system

The finite element model of unbalanced single disk rotor system is established. Fig. 9 shows the schematic of the model. In order to explore the influence of the support stiffness on the first-order speed of the rotor system, the first-order speed is calculated by changing the stiffness coefficient of the support in the model. Fig. 10 shows the distribution of the first-order speed against the stiffness coefficient at the support without damping.

Fig. 10 indicates that the first-order speed of the rotor system increases with the increases in support stiffness. Moreover, it is observed that when the support stiffness exceeds 1×10^7 N/m, the first-order speed of the rotor system no longer increases with the increase in the support stiffness. It is concluded that the design stiffness coefficient of GISFD should be less than 1×10^7 N/m to provide elastic support for the rotor system.

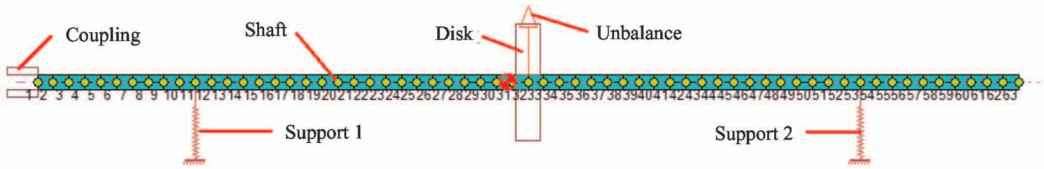

Fig. 9 Finite element model of the rotor system with an unbalanced single disk

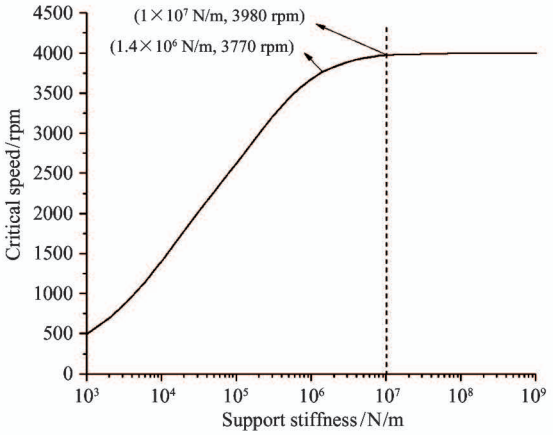

Fig. 10 Distribution of the first-order speed against the stiffness coefficient of the support

Fig. 3(a) indicates that the stiffness coefficient of GISFD is 1.4×10^6 N/m. However, the stiffness coefficient of the rolling bearing used in the rotor system support is generally 1×10^8 N/m, which is far greater than that of GISFD. When GISFD is applied to the rotor system, the supporting stiffness of the rotor is about 1.4×10^6 N/m. Fig. 10 indicates that the first-order speed of the rotor reduces to 3770 rpm. Therefore, the proposed damper meets the design requirements, which provides elastic support for the rotor system.

4.2 Investigation on the damping performance of GISFD

In order to investigate the influence of GISFD on the unbalanced response of the rotor system, experiments are conducted on the rotor system with the GISFD and with no damper. Prior to the experiment, a mass of $m = 0.46$ g is added to the counterweight hole (at radius of $r = 30$ mm) at the 0° phase of the disk. The applied unbalanced weight is set to $u = 13.8$ g · mm. During the experiment, two types of supports, including the rigid support (i.e. no damper) and GISFD support, are utilized to compare the variation of the unbalanced response of the rotor system with and without the damper.

In order to explore the effect of different viscosity damping fluids on GISFD damping performance, the silicone oil with different kinematic viscosity is injected into GISFD as the damping fluid. Accordingly, the influence of GISFD with different damping fluids on the unbalanced response of the rotor system can be investigated. The silicone oil is a polydimethylsiloxane polymer with high viscosity and well thermal stability.

It should be indicated that 4 types of silicone oil with kinematic viscosity coefficients of $v = 3.5$ cm^2/s, 5.0 cm^2/s, 10.0 cm^2/s and 30.0 cm^2/s are employed in GISFD support in the experiment.

In the test, the rotor speed is increased from 200 rpm to 5500 rpm. Then the rotor speed and the peak-peak value of the vibrational amplitude of the rotor near the disk are measured and recorded. Fig. 11 illustrates the unbalanced response curves of the rotor in the horizontal and vertical directions with different support conditions. Table 3 presents the peak-peak amplitudes in the horizontal and vertical directions at the critical

speed at different support conditions, respectively. It is observed that compared with rigid support, the effect of suppressed vibration of GISFD support is calculated.

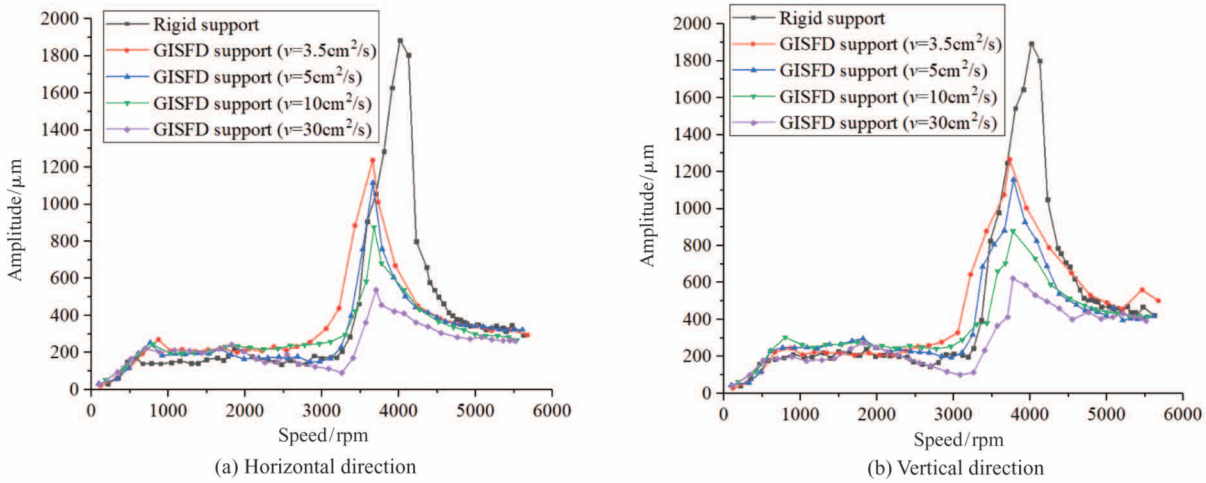

Fig. 11 Distributions inunbalanced response of the rotor near disk at different support conditions

Table 3 Critical speeds and peak-peak amplitudes at different support conditions

Condition	Measurement direction	Critical speed/rpm	Amplitude/μm	Vibration reduction/%
Rigid support	Horizontal	4014	1885	-
	Vertical	4014	1894	-
GISFD support (v = 3.5 cm^2/s)	Horizontal	3659	1239	34.27
	Vertical	3729	1266	33.16
GISFD support (v = 5.0 cm^2/s)	Horizontal	3663	1116	40.80
	Vertical	3781	1157	38.91
GISFD support (v = 10.0 cm^2/s)	Horizontal	3676	877	53.47
	Vertical	3773	878	53.64
GISFD support (v = 30.0 cm^2/s)	Horizontal	3703	537	71.51
	Vertical	3773	621	67.21

Fig. 11 indicates that the vibration of the unbalanced response of the rotor is effectively suppressed after the installation of GISFD with different viscosity damping fluids. Table 3 shows that when the rigid support (i.e. case with no damper) is adopted, the critical speed of the rotor in the horizontal and vertical directions is about 4000 rpm, while the corresponding peak-peak amplitudes of the rotor in the horizontal and vertical directions at the critical speed are 1885 μm and 1894 μm, respectively. When GISFD is applied, the critical speed of rotor in horizontal and vertical direction is about 3700 rpm, while the corresponding peak-peak amplitudes at the critical speed decrease as the viscosity of the damping fluid in GISFD increases. It is observed that when the kinematic viscosity coefficient of the damping fluid is set to v = 30.0 cm^2/s, the vibration amplitude of the rotor at the critical speed is the smallest, and the corresponding peak-peak amplitudes in the horizontal and vertical directions are 537 μm and 621 μm, respectively.

Obtained experimental results show that GISFD not only reduces the critical speed of the rotor, but also improves the rotor system damping so that it improves the damping ratio of the rotor system and effectively suppresses the vibration of the rotor system. It is concluded that in a certain range, the greater the kinematic viscosity of the damping fluid, the greater the damping coefficient of the damper, and the better damping performance of the GISFD. When the silicone oil with kinematic viscosity coefficients v = 30.0 cm^2/s is employed as the damping fluid, the vibration reduction of the GISFD in the studied case is as high as 71.51%.

4.3 Unbalanced response of the rotor supported by GISFD at different unbalance quantities

In order to investigate the unbalanced response of GISFD rotor system at different unbalanced conditions, experiments are carried out. During the experiment,

GISFD support is applied to the rotor system, while the silicone oil with kinematic viscosity $v = 10.0\ \mathrm{cm^2/s}$ is employed as the damping fluid. Then the weight block with different masses, ranging from $m = 0.46$ g to $m = 1.67$ g, is added to the counterweight hole (at radius of $r = 30$ mm) at 0° phase of the disk. In this research, four weights $m = 0.46$ g, 0.58 g, 0.99 g and 1.67 g are utilized, where the corresponding unbalances are $u = 13.8$ g · mm, 17.4 g · mm, 29.7 g · mm and 50.1 g · mm, respectively. The experiment is carried out to investigate the unbalanced response of the rotor system.

In the test, the rotor speed increases from 200 rpm to 5500 rpm. The rotor speed and the peak-peak value of the vibrational amplitude of the rotor near the disk are measured and recorded. Fig. 12 illustrates the unbalanced response curves of the rotor in the horizontal and vertical directions at different unbalance values. Moreover, the curves of the unbalance values and the peak-peak amplitude are shown in Fig. 13.

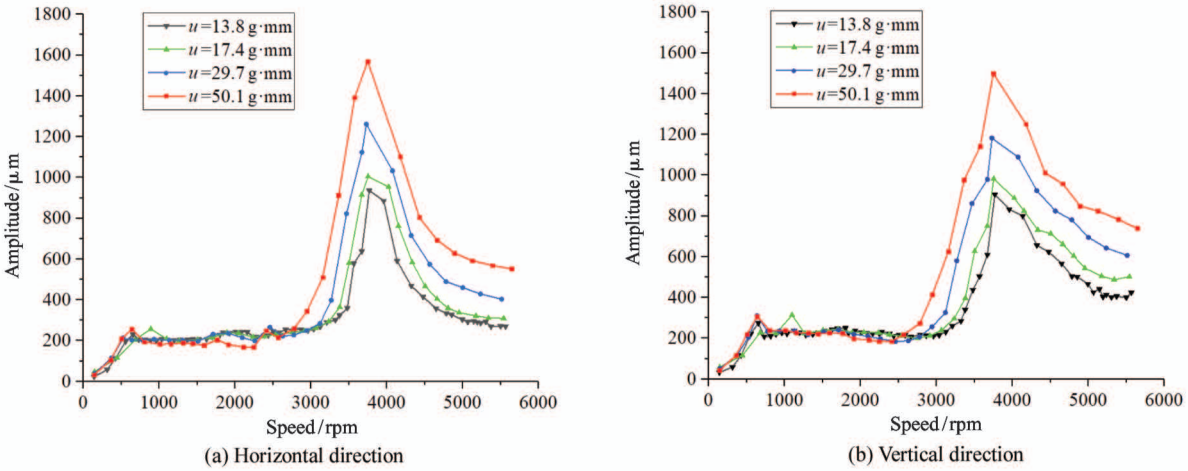

Fig. 12 Distribution of unbalanced response of the rotor near disk at different unbalance conditions

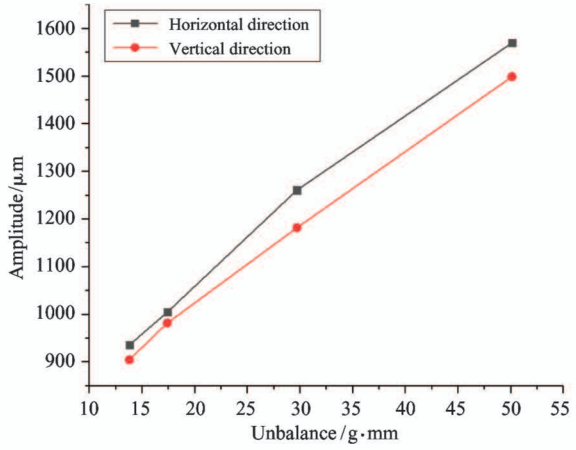

Fig. 13 Curve of the unbalance and the peak-peak amplitude

Fig. 12 indicates that when the speed of the rotor is close to the critical speed (i. e. about 3700 rpm), the corresponding peak-peak values of amplitude reach the maximum value. On the other hand, when the rotor speed is far greater than the critical speed, the rotor has the phenomenon of automatic centering, and the corresponding peak-peak values of amplitude obviously decrease and tend to be stable. Since GISFD reduces the vibration in the rotor system, the rotor system can pass through the critical speed safely and stably even if the system has a large unbalance.

It can be found from Fig. 12 that under the GISFD supported condition, when the rotor system is configured with $u = 50.1$ g · mm, the amplitude of the rotor near the critical speed is approximately 1600 μm. As can be seen from Table 3, under the condition that the corresponding unbalance is $u = 13.8$ g · mm, the amplitude of the rigid supported rotor system is approximately 1900 μm. It can be seen that GISFD can effectively reduce the sensitivity of the rotor system to unbalance.

Fig. 13 shows that with the increase of unbalance, the corresponding amplitude of response becomes larger, which is linear correlation.

Experimental results show that GISFD has good damping performance and stability. GISFD has excellent linear damping characteristics and reduces the sensitivity of the rotor system to the unbalanced mass.

5 Conclusions

In this research, a G-type integral squeeze film damper (GISFD) is proposed for the first time. GISFD can effectively improve the nonlinear problem of traditional SFD and the stability of the rotor system. Moreover, GISFD has superiorities including simple structure, convenient assembly and excellent damping perform-

ance. Theoretical analysis and experimental verification are performed to investigate GISFD and its effect on suppressing the unbalanced response vibration of the rotor system. The main conclusions are the followings.

(1) The simulation results show that the proposed damper not only meets the design requirements, but also has reasonable structural strength.

(2) An unbalance of $u = 13.8\ \mathrm{g \cdot mm}$ is added to the disk, and experiments are performed to investigate the unbalanced response of the rotor system. The experimental results show that GISFD can effectively suppress the unbalanced response vibration of the rotor system.

(3) Through the experimental verification, it is observed that in a certain viscosity range, the larger the kinematic viscosity coefficient of the damping fluid, the better the effect of GISFD on suppressing the unbalanced response vibration of the rotor system. When the silicone oil with kinematic viscosity coefficients $v = 30.0\ \mathrm{cm^2/s}$ is employed as the damping fluid, the vibration reduction of GISFD is approximately 71.51%.

(4) The conducted experiment verifies that GISFD has good linear damping characteristics and reduces the sensitivity of the rotor system to the unbalanced mass.

References

[1] Vance J, ZeidanF, Murphy B. Machinery Vibration and Rotor Dynamics[M]. Hoboken: John Wiley and Sons, 2010: 72-83

[2] Meeus H, Fiszer J, Van De Velde G, et al. Dynamic performance of a squeeze film damper with a cylindrical roller bearing under a large static radial loading range [J]. *Machines*, 2019, 7:1-14

[3] Mohan S, Hahn E J. Design of squeeze film damper supports for rigid rotors[J]. *Journal of Engineering for Industry*, 1974, 96(3):976-982

[4] Gunter E J, Barrett L E, Allaire P E. Design of nonlinear squeeze-film dampers for aircraft engines[J]. *Journal of Lubrication Technology*, 1977, 99(1):57-64

[5] Botman M. Experiments on oil-film dampers for turbomachinery[J]. *Journal of Engineering for Power*, 1976, 98(3):393-399

[6] Inayat-Hussain J I, Mureithi N W. Transitions to chaos in squeeze-film dampers[J]. *Communications in Nonlinear Science and Numerical Simulation*, 2006, 11(6):721-744

[7] Zhao J Y, Hahn E J. Subharmonic, quasi-periodic and chaotic motions of a rigid rotor supported by an eccentric squeeze film damper[J]. *Proceedings of the Institution of Mechanical Engineers Part C Journal of Mechanical Engineering Science*, 1993, 207(6):383-392

[8] Andres L A S, Vance J M. Effect of fluid inertia on the performance of squeeze film damper supported rotors[J]. *Journal of Engineering for Gas Turbines and Power*, 1988, 110(1):51-57

[9] Zhou H L, Luo G H, Chen G, et al. Analysis of the nonlinear dynamic response of a rotor supported on ball bearings with floating-ring squeeze film dampers[J]. *Mechanism and Machine Theory*, 2013, 59:65-77

[10] Zapoměl J, Ferfecki P, Kozánek J. Modelling of magnetorheological squeeze film dampers for vibration suppression of rigid rotors[J]. *International Journal of Mechanical Sciences*, 2017, 127(1):191-197

[11] Han Z F, Ding Q, Zhang W. Dynamical analysis of an elastic ring squeeze film damper-rotor system[J]. *Mechanism and Machine Theory*, 2019, 131:406-419

[12] Chang-Jian C W, Yau H T, Chen J L. Nonlinear dynamic analysis of a hybrid squeeze-film damper-mounted rigid rotor lubricated with couple stress fluid and active control [J]. *Applied Mathematical Modelling*, 2010, 34(9): 2493-2507

[13] Memmott E A. The stability of centrifugal compressors by applications of tilt-pad seals[C]// The 8th International Conference on Vibration in Rotating Machinery, Swansea, UK, 2004: 81-90

[14] Zhao J Y, Linnett I W, Mclean L J. Unbalance response of a flexible rotor supported by a squeeze film damper [J]. *Journal of Vibration and Acoustics*, 1998, 120(1): 32-38

[15] He F, Dousti S, Allaire P, et al. Squeeze film damper effect on vibration of an unbalanced flexible rotor using harmonic balance method[J]. *Journal of Engineering Science and Technology*, 2017, 12(3):667-685

[16] Huang X J, He L D, Wang C. Research on suppress vibration of rotor misalignment with shear viscous damper [J]. *High Technology Letters*, 2015, 21(2):239-243

[17] Ferfecki P, Zapoměl J, Marek M. Multi-physical analysis of the forces in the flexible rotor supported by the magnetorheological squeeze film dampers[J]. *Advances in Mechanism Design II*, 2017, 44:89-95

[18] Zapomel J, Ferfecki P, Forte P. A computational investigation of the steady state vibrations of unbalanced flexibly supported rigid rotors damped by short magnetorheological squeeze film dampers[J]. *Journal of Vibration and Acoustics*, 2013, 135(6):doi:10.1115/1.4024881

[19] Zhao J H, Wang Q, Zhang B, et al. Research on static bearing characteristics of magnetic-liquid double suspension bearing[J]. *High Technology Letters*, 2019, 25(4): 434-442

[20] Kasarda M E F, Mendoza H, Kirk R G, et al. Reduction of subsynchronous vibrations in a single-disk rotor using an active magnetic damper[J]. *Mechanics Research Communications*, 2004, 31(6):689-695

[21] ErtasB, Delgado A, Moore J. Dynamic characterization of an integral squeeze film bearing support damper for a supercritical CO_2 expander [C]// Proceedings of ASME Turbo Expo: Turbomachinery Technical Conference and Exposition, Charlotte, USA, 2017: 1-9

Yan Wei, born in 1994. He is studying for his Ph. D degree in Diagnosis and Self-recovery Engineering Research Center of Beijing University of Chemical Technology. He received his M. S. degree in Mechanical Engineering of Liaoning Technical University in 2018 and his B. S. degree in Process Equipment and Control Engineering of Jilin Institute of Chemical Technology in 2016. His research interests are vibration control of pipeline and rotating machinery.